

# Real-Time Needle Guidance with Photoacoustic and Laser-Generated Ultrasound Probes

Richard J. Colchester,<sup>a</sup> Charles A. Mosse,<sup>a</sup> Daniil I. Nikitichev,<sup>a</sup> Edward Z. Zhang,<sup>a</sup> Simeon West,<sup>b</sup> Paul C. Beard,<sup>a</sup> Ioannis Papakonstantinou,<sup>c</sup> Adrien E. Desjardins<sup>a,\*</sup>

<sup>a</sup>Department of Medical Physics and Biomedical Engineering, University College London, Malet Place Engineering Building, London WC1E 6BT, United Kingdom

<sup>b</sup>University College Hospital, 235 Euston Rd, London NW1 2BU, United Kingdom

<sup>c</sup>Department of Electronic and Electrical Engineering, University College London, Roberts Building, London WC1E 7JE, United Kingdom

## ABSTRACT

Detection of tissue structures such as nerves and blood vessels is of critical importance during many needle-based minimally invasive procedures. For instance, unintentional injections into arteries can lead to strokes or cardiotoxicity during interventional pain management procedures that involve injections in the vicinity of nerves. Reliable detection with current external imaging systems remains elusive. Optical generation and reception of ultrasound allow for depth-resolved sensing and they can be performed with optical fibers that are positioned within needles used in clinical practice. The needle probe developed in this study comprised separate optical fibers for generating and receiving ultrasound. Photoacoustic generation of ultrasound was performed on the distal end face of an optical fiber by coating it with an optically absorbing material. Ultrasound reception was performed using a high-finesse Fabry-Pérot cavity. The sensor data was displayed as an M-mode image with a real-time interface. Imaging was performed on a biological tissue phantom.

**Keywords:** Photoacoustic, laser-generated ultrasound, needle guidance

**Address all correspondence to:** Adrien E. Desjardins; Tel: +44 20 76790300; Email: [a.desjardins@ucl.ac.uk](mailto:a.desjardins@ucl.ac.uk)

## 1. INTRODUCTION

In many needle-based interventional pain management procedures, external X-ray fluoroscopy and ultrasound imaging systems that generate images from outside the patient provide insufficient information for reliably detecting tissue targets or critical structures. For instance, nerve targets are not directly visible with X-ray fluoroscopy<sup>1</sup> and it is often challenging to visualize them with ultrasound imaging<sup>2</sup>. Unintentional injections into arteries can lead to severe complications, including strokes or death<sup>3</sup>.

Sensors integrated into the needle tip can provide information about surrounding tissues that is complementary to the images from external imaging systems. A wide range of optical and non-optical sensors have been integrated into needles. In the context of interventional pain management, optical reflectance spectroscopy probes that are integrated into needle stylets can provide optical contrast for changes in lipid and hemoglobin concentrations that can be used to identify contact with nerves and entry into blood vessels, respectively<sup>4,5</sup>. These probes typically have separate optical fibers for delivering light to tissue and for receiving scattered light. A prominent limitation is that the depth in tissue from which information is obtained decreases with the distance between the optical fibers that deliver and receive light. As a result, these probes do not lend themselves well to obtaining depth-resolved information. A needle probe with optical coherence tomography provided depth-resolved information about nerves with micron-scale resolution<sup>6</sup>, but its sensing depth in tissue was limited to around 1 mm.

In this study, a needle probe that performed pulse-echo ultrasound was developed. Ultrasound was generated at a composite coating in the probe that absorbed incident excitation light. Ultrasound reception was performed with an optical fiber sensor with a high-finesse Fabry-Pérot (F-P) cavity. M-mode imaging was performed on human fingertips in water.

## 2. MATERIALS AND METHODS

### 2.1 Needle probe

The needle stylet was designed to be positioned within a 16 gauge injection needle (Figure 1). It comprised two multi-mode fibers (core/cladding: 200/208  $\mu\text{m}$ ): one for transmitting ultrasound for pulse-echo ultrasound sensing and another for transmitting light into the sample for photoacoustic sensing. The latter fiber was not used, as photoacoustic sensing was not performed in this study. Additionally, it comprised a single-mode fiber (SMF-28e) for receiving ultrasound. Each optical fiber was positioned within 24 gauge stainless steel hypotubes (O.D./I.D.: 570/340  $\mu\text{m}$ ), with the distal ends of the fibers slightly recessed from the distal end of the tubing ( $\sim 50$  to 200  $\mu\text{m}$  behind the back of the bevelled tip). The tubing provided acoustic isolation between the transmitting and receiving fibers, and mechanical protection for the fibers. At the proximal end, the needle stylet had a side-arm fitting with one port for the optical fibers and a luer connector that allowed for fluid to be injected through the hypotubes.

The optical fiber that transmitted ultrasound had a composite coating on its end face to absorb incident excitation light. The coating comprised polydimethylsiloxane (PDMS) with integrated multi-walled carbon nanotubes (CNTs). The PDMS served as an elastomer with a high thermal expansion coefficient; the CNTs, as optical absorbers. The CNTs were functionalized to allow for their dissolution in a solvent of PDMS. The method for creating this composite and its method of application were similar to those previously described<sup>7</sup>.

The optical fiber that received ultrasound had a (F-P) cavity on the distal end. As previously described by Zhang et al.<sup>8</sup>, the F-P cavity comprised two dielectric mirror coatings with an optical epoxy spacer in between (approximate thickness: 20  $\mu\text{m}$ ). The first mirror coating was deposited directly onto the fiber end face cleaved at normal incidence; the other, on the distal surface of the polymer spacer. As mechanical protection for the distal dielectric mirror coating, a Parylene-C coating with a thickness of 10  $\mu\text{m}$  was applied.

### 2.2 Console

Excitation light for ultrasound generation was provided by a fiber coupled Nd:YAG laser with a wavelength of 1064 nm, a pulse width of 2 ns, and a repetition rate of 100 Hz (SPOT-10-500-1064, Elforlight, UK). The fluence of the excitation light, as measured at the distal end face of the optical fibers, was 45  $\text{mJ}/\text{cm}^2$ .

For ultrasound sensing, the F-P cavity was interrogated using a continuous wave, tunable laser (Tunics T100S-HP CL, Yenista Optics, France) that operated at wavelengths in the range of 1500 to 1600 nm. The interrogation wavelength was chosen so that it corresponded to the peak derivative of the transfer function, to provide optimum sensitivity to impinging ultrasound waves<sup>9</sup>. Light reflected from the F-P cavity was directed to a 50 MHz photodiode-transimpedance amplifier unit via an optical circulator. This amplifier unit had a low-frequency ( $< 50$  kHz) output that was acquired at 1 MS/s with a 16-bit digitizer (PCI-6251, National Instruments, UK) to record the F-P cavity transfer function. A high-frequency output ( $> 500$  kHz) was digitized at 100 MS/s with a 14-bit digitizer (PCI-5142, National Instruments, UK) in combination with a 48 MHz low-pass analog filter (BLP-50+, Mini-Circuits, NY, USA) to record modulations of the reflected light produced by incident ultrasound waves. The ultrasound bandwidth of the sensor was approximately 20 MHz. Signal averaging was not performed.

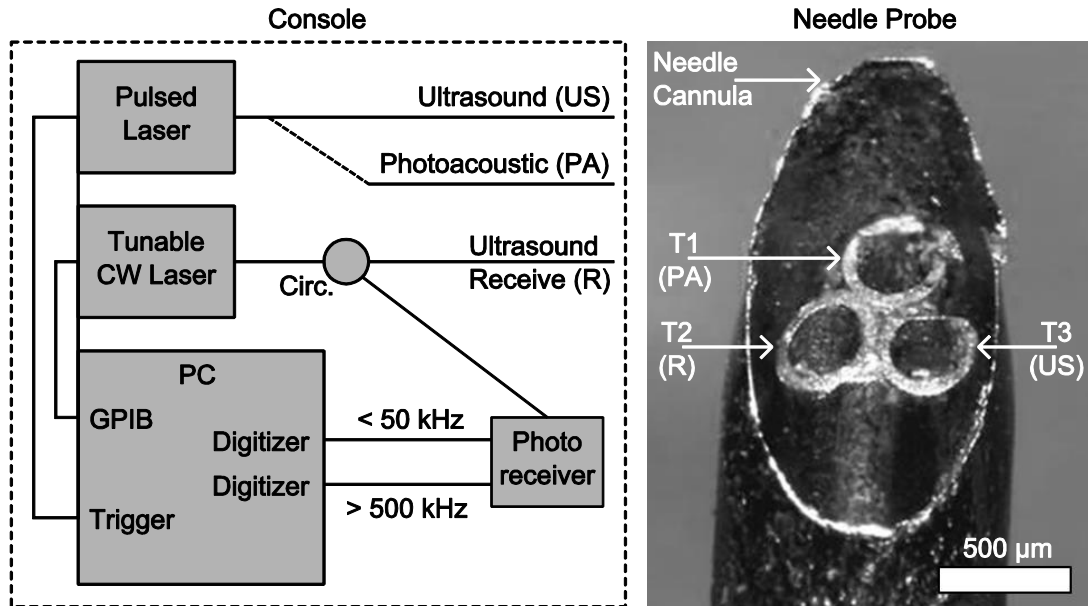


Figure 1. The needle probe (right) comprised a removable stylet made from three hypotubes: one with a bare fiber for photoacoustic sensing (T1), a second for transmitting ultrasound for pulse-echo sensing (T3), and a third for receiving ultrasound (T2). The fibers are recessed in the tubes so that they are not visible in the photograph. The probe was interrogated by a console (left) that delivered pulsed light to the fibers in T1 and T3, and continuous (CW) light from a wavelength-tunable laser to the fiber in T2. Light reflected from the Fabry-Pérot cavity at the distal end of the ultrasound-receiving fiber was directed via a circulator (Circ.) to a photo-receiver with a low-frequency output used for tuning the CW laser and a high-frequency output that served as the ultrasound signal.

### 2.3 Signal Processing and Display

A digital high-pass frequency filter (4<sup>th</sup> order Butterworth; cut-off: 5 MHz) was applied prior to cross-talk removal to reduce noise. Envelope detection with the Hilbert transform and logarithmic transformation were performed prior to display.

During pulse-echo ultrasound sensing, propagation of ultrasound directly between the ultrasound transmitter and receiver and reflections within the metal tubes resulted in cross-talk artifacts that manifested as a prominent background. Two signal processing steps were performed to remove them. The first step involved dynamic background subtraction using a general linear model, in which the background of an A-line was modeled as a linear combination of three components: a) a constant vector; b) the mean of a previous set of A-lines; c) the temporal derivative of the mean. The implementation of this general linear model approach was described in detail by Colchester et al<sup>10</sup>. The second image processing step involved multiplying the frequency-filtered digitized signal by a depth-dependent gain factor,  $g$ . This gain factor varied with the temporal sample index  $i$ , as follows:

$$g(i) = \min(i/m, 1)^\alpha,$$

where  $m$  is less than the number of samples per A-line, and  $\alpha$  is a positive real number. The choices  $m = 100$  and  $\alpha = 2.0$  were made empirically, so that a balance between cross-talk artifact reduction and signal preservation was achieved.

Real-time signal processing and display was performed using a custom program that was written in Labview (Austin, TX, USA) and run on a PC (HP Z220 Workstation; 3.4 GHz CPU, 12 GB RAM). The display consisted of a streaming M-mode image, with depth on the vertical axis and time on the horizontal axis. Averaging of signals across consecutive A-lines was not performed for M-mode imaging.

## 2.4 M-mode imaging

To assess the potential of the probe to visualize moving tissue, the needle probe was placed in a water bath facing the fingertips of a human hand. The fingertips were freely moved relative to the needle probe and M-mode images were acquired and displayed in real-time.

## 3. RESULTS

### 3.1 M-mode imaging

With pulse-echo ultrasound sensing, human fingertips in water could clearly be visualized as an M-mode image (Figure 4). Signal from within tissue was observed at depths in tissue exceeding 0.5 cm, and cross-talk artifacts were largely absent.

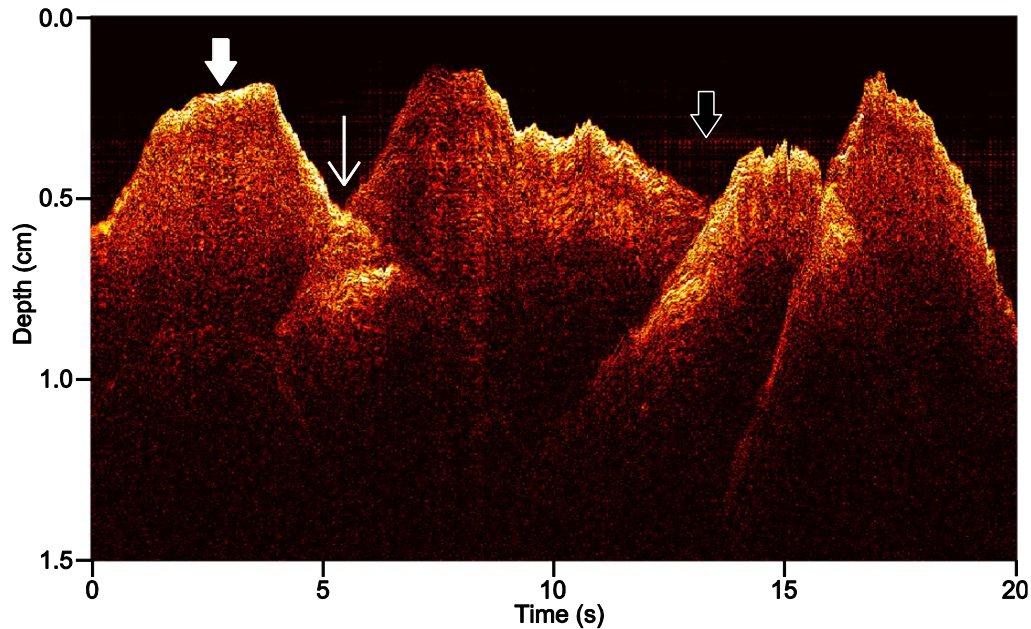


Figure 2. Human fingertips in water, displayed as an M-mode ultrasound image. As the fingertips were freely translated across the distal end of the probe, the skin-water interface (wide solid arrow) and the junctions between adjacent fingers (thin arrow) were apparent. Cross-talk was apparent to a limited extent at depths in the vicinity of 0.4-0.5 cm (wide outlined arrow).

## 4. DISCUSSION

The needle probe developed in this study was, to the authors' knowledge, the first that allowed for all-optical real-time pulse-echo ultrasound sensing. While needle probes with electrical transmission and reception of ultrasound have previously been implemented to guide epidural steroid injections<sup>11</sup>, optical transmitters and receivers are particularly well suited to needle-based probes. Indeed, the small diameter of the optical ultrasound sensor could be compatible with small-diameter needles (e.g. 20 to 22 gauge) that are often used in interventional pain management procedures.

M-mode imaging of human fingertips moving in water provided an initial indication that pulse-echo ultrasound sensing in a needle can be performed all-optically with sufficient sensitivity to resolve tissue-water interfaces, without signal averaging. As such, it set the stage for imaging in more realistic models for interventional pain management, which could include nerves and blood vessels *in situ*. Future iterations of the probe could deliver light directly to tissue for photoacoustic sensing, to provide direct contrast for haemoglobin and lipids.

## 5. CONCLUSION

This study demonstrated that pulse-echo ultrasound sensing can be obtained all-optically in an injection needle. Real-time M-mode imaging with this probe has strong potential to provide information for guiding interventional pain management procedures that is complementary to external imaging modalities.

## 6. ACKNOWLEDGMENTS

This work was supported in part by the EPSRC under Grant No. EP/J010952/1, by the European Research Council under ERC-2012-StG Proposal 310970, European Union project FAMOS (FP7 ICT, Contract 317744), and by the University College London-Cambridge University Photonic Systems Development Centre for Doctoral Training.

## 7. REFERENCES

- [1] Balthasar, A., Desjardins, A. E., van der Voort, M., Lucassen, G. W., Roggeveen, S., Wang, K., Bierhoff, W., Kessels, A. G. H., Sommer, M., et al., "Optical detection of vascular penetration during nerve blocks: an in vivo human study.," *Reg. Anesth. Pain Med.* **37**(1), 3–7 (2011).
- [2] Balthasar, A., Desjardins, A. E., van der Voort, M., Lucassen, G. W., Roggeveen, S., Wang, K., Bierhoff, W., Kessels, A. G. H., van Kleef, M., et al., "Optical detection of peripheral nerves: an in vivo human study.," *Reg. Anesth. Pain Med.* **37**(3), 277–282 (2012).
- [3] Smuck, M., Tang, C.-T., Fuller, B. J., "Incidence of Simultaneous Epidural and Vascular Injection During Cervical Transforaminal Epidural Injections," *Spine (Phila. Pa. 1976)*. **34**(21), 751–755 (2009).
- [4] Brynolf, M., Sommer, M., Desjardins, A. E., van der Voort, M., Roggeveen, S., Bierhoff, W., Hendriks, B. H. W., Rathmell, J. P., Kessels, A. G. H., et al., "Optical detection of the brachial plexus for peripheral nerve blocks: an in vivo swine study.," *Reg. Anesth. Pain Med.* **36**(4), 350–357 (2011).
- [5] Desjardins, A. E., van der Voort, M., Roggeveen, S., Lucassen, G., Bierhoff, W., Hendriks, B. H. W., Brynolf, M., Holmström, B., "Needle stylet with integrated optical fibers for spectroscopic contrast during peripheral nerve blocks.," *J. Biomed. Opt.* **16**(7), 077004 (2011).
- [6] Raphael, D. T., Yang, C., Tresser, N., Wu, J., Zhang, Y., Rever, L., "Images of spinal nerves and adjacent structures with optical coherence tomography: preliminary animal studies.," *J. Pain* **8**(10), 767–773 (2007).
- [7] Colchester, R. J., Mosse, C. a., Bhachu, D. S., Bear, J. C., Carmalt, C. J., Parkin, I. P., Treeby, B. E., Papakonstantinou, I., Desjardins, A. E., "Laser-generated ultrasound with optical fibres using functionalised carbon nanotube composite coatings," *Appl. Phys. Lett.* **104**(17), 173502 (2014).
- [8] Zhang, E. Z., Beard, P. C., "A miniature all-optical photoacoustic imaging probe," *Proc. SPIE* **7899**, A. A. Oraevsky and L. V. Wang, Eds., 78991F–1– 78991F–6 (2011).
- [9] Zhang, E., Laufer, J., Beard, P., "Backward-mode multiwavelength photoacoustic scanner using a planar Fabry-Perot polymer film ultrasound sensor for high-resolution three-dimensional imaging of biological tissues.," *Appl. Opt.* **47**(4), 561–577 (2008).
- [10] Colchester, R. J., Zhang, E. Z., Mosse, C. A., Beard, P. C., Papakonstantinou, I., Desjardins, A. E., "Broadband miniature optical ultrasound probe for high resolution vascular tissue imaging (in press)," *Biomed. Opt. Express*.
- [11] Chiang, H. K., Zhou, Q., Mandell, M. S., Tsou, M.-Y., Lin, S.-P., Shung, K. K., Ting, C.-K., "Eyes in the needle: novel epidural needle with embedded high-frequency ultrasound transducer — epidural access in porcine model," *Anesthesiology* **114**(6), 1320–1324 (2011).